ANTIOXIDANTS & REDOX SIGNALING
Volume 14, Number 1, 2011

DOI: 10.1089/ars.2009.3068

FORUM ORIGINAL RESEARCH COMMUNICATION

Stabilization of α-Conotoxin AuIB: Influences of Disulfide Connectivity and Backbone Cyclization

Erica S. Lovelace,[1] Sunithi Gunasekera,[1] Charlotta Alvarmo,[1] Richard J. Clark,[1] Simon T. Nevin,[2] Anton A. Grishin,[2,3] David J. Adams,[2,3] David J. Craik,[1] and Norelle L. Daly[1]

Abstract

α-Conotoxins are peptides isolated from the venom ducts of cone snails that target nicotinic acetylcholine receptors (nAChRs). They are valuable pharmacological tools and have potential applications for treating a range of conditions in humans, including pain. However, like all peptides, conotoxins are susceptible to degradation, and to enhance their therapeutic potential it is important to elucidate the factors contributing to instability and to develop approaches for improving stability. AuIB is a unique member of the α-conotoxin family because the nonnative "ribbon" disulfide isomer exhibits enhanced activity at the nAChR in rat parasympathetic neurons compared with the native "globular" isomer. Here we show that the ribbon isomer of AuIB is also more resistant to disulfide scrambling, despite having a nonnative connectivity and flexible structure. This resistance to disulfide scrambling does not correlate with overall stability in serum because the ribbon isomer is degraded in human serum more rapidly than the globular isomer. Cyclization *via* the joining of the N- and C-termini with peptide linkers of four to seven amino acids prevented degradation of the ribbon isomer in serum and stabilized the globular isomers to disulfide scrambling. The linker length used for cyclization strongly affected the relative proportions of the disulfide isomers produced by oxidative folding. Overall, the results of this study provide important insights into factors influencing the stability and oxidative folding of α-conotoxin AuIB and might be valuable in the design of more stable antagonists of nAChRs. *Antioxid. Redox Signal*. 14, 87–95.

Introduction

α-CONOTOXINS are small disulfide-rich peptide toxins isolated from the venoms of predatory marine snails of the *Conus* genus (1, 13, 25, 32). They are generally 12–19 amino acids in size and specifically inhibit muscle and neuronal nicotinic acetylcholine receptor (nAChR) subtypes (14). Their potency and selectivity make them valuable tools in understanding the mechanisms involved in ligand–receptor interactions (11) and also engender them with a range of potential therapeutic applications, most notably for the treatment of chronic pain (5, 22). However, like many peptides, conotoxins are potentially limited in their use as therapeutics by their susceptibility to proteolytic degradation and/or disulfide bond shuffling, which produces inactive derivatives (3). Such limitations can be overcome *via* appropriate delivery routes or *via* chemical modification to stabilize them. For instance, a synthetic version of ω-conotoxin MVIIA ("Prialt"), which is marketed for the treatment of chronic pain, is infused intrathecally to exert its biological effects directly at the site of action (20, 27). Similarly, a modified version of χ-conotoxin MrIA, Xen2174, is currently undergoing clinical trials for pain *via* intrathecal delivery. Xen2174 contains a modified N-terminus, which ameliorates the aforementioned stability problems (7). Thus, it is of significant interest to determine the factors that influence stability, which will enable the design of novel conotoxins with enhanced therapeutic stability.

Recently, backbone cyclization has been used as a method to improve the stability of conotoxins (8, 23). Artificially cyclized derivatives of the naturally occurring α-conotoxins MII (7, 8), ImI (4), and χ-conotoxin MrIA (23) all have improved stability over their linear parent peptides. However, it is of interest to determine if factors such as the amino acid sequence, three-dimensional (3D) structure, or cysteine spacing influence the effectiveness of cyclization. In the present study we cyclized α-conotoxin AuIB because it has different cysteine spacing and it significantly differs in sequence from MII, ImI, and MrIA.

α-Conotoxin AuIB, originally isolated from the cone snail *Conus aulicus*, comprises 15 amino acid residues and targets

[1]Division of Chemistry and Structural Biology, Institute for Molecular Bioscience and [2]Queensland Brain Institute, The University of Queensland, Brisbane, Australia.
[3]Health Innovations Research Institute, RMIT University, Melbourne, Australia.

mainly the $\alpha 3\beta 4$ subtype of the nAChR (24). α-Conotoxins are classified based on the number of residues within their two intercysteine loops, and AuIB was the first example of a 4/6 spacing (*i.e.*, having four residues in the first loop and six in the second loop) in this family of conotoxins. Other 4/6 conotoxins have since been found, including Pu1.2, Lp1.6a, and Lp1.6b, but the number of examples with this cysteine spacing is still limited (35). The 3D structures of both the globular (Cys^{I}-Cys^{III}, Cys^{II}-Cys^{IV}) and ribbon (Cys^{I}-Cys^{IV}, Cys^{II}-Cys^{III}) isomers of AuIB have been determined using nuclear magnetic resonance (NMR) spectroscopy (12) and are shown in Figure 1. The globular isomer has a well-defined structure displaying the classic α-conotoxin fold, with the major element of secondary structure being an α-helix centered around Cys^{III} (28). By contrast, the ribbon isomer is poorly defined and lacks regular secondary structure. Despite this lack of structure, the ribbon isomer inhibits neuronal nAChRs in rat parasympathetic ganglia with a potency of ~10-fold greater than the globular isomer (12). This finding is unusual for α-conotoxins because the globular isomer is typically the native form in the venom and is usually the most potent bioactive conformation. In another illustration of the complexity of the pharmacology of α-conotoxins, it has been reported that the globular form of AuIB is more active than the ribbon isomer on oocyte-expressed $\alpha 3\beta 4$ receptors (30), but this has recently been shown to be dependent on the stoichiometry of receptor subunits (16). Further, it is possible there are other targets for AuIB that have not yet been identified.

In the present study we analyzed the disulfide bond stability (*i.e.*, susceptibility to disulfide scrambling) as well as the overall stability of AuIB and a range of cyclic analogs in serum. We found that the acyclic ribbon isomer is more stable in the presence of glutathione than the native globular isomer. By contrast, the ribbon form is rapidly degraded in human serum, presumably *via* proteolysis, whereas the globular isomer remains intact. Backbone cyclization prevented degradation of the ribbon isomer in human serum, providing strong support for the concept that cyclization is a valuable general technique for stabilizing conotoxin peptides.

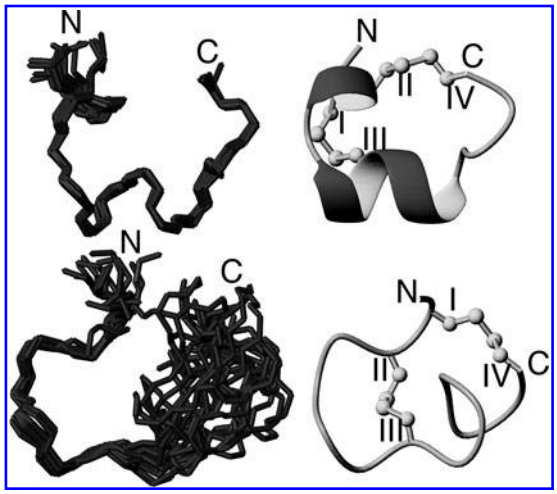

FIG. 1. Three-dimensional structures of AuIB. An overlay of the 20 lowest energy structures is given on the left and the secondary structure is highlighted on the right. The globular isomer (PDB code 1mxn) is shown on the top and the ribbon (PDB code 1mxp) on the bottom.

Materials and Methods

Peptide synthesis

All AuIB analogs were synthesized, oxidized, and cyclized according to previously established protocols used by Dutton *et al.* (2002) and Clark *et al.* (2005) (8, 12). Oxidation and thiazip cyclization were performed in a single step in 20% isopropanol/80% 100 m*M* ammonium bicarbonate (pH 7.5) at room temperature for 24 h at a peptide concentration of 0.8 mg/ml. The conditions for oxidative folding were based on previous folding studies on the linear peptides (12). Peptides were purified by high-performance liquid chromatography (HPLC) using a Vydac C_{18} column at a 1% gradient (increasing 1% solvent B per minute). Solvent A is 0.1% trifluoroacetic acid (TFA) in water and solvent B is 0.05% TFA in 90% acetonitrile. The purity of the products was verified by using analytical C_{18} HPLC and by electrospray mass spectrometry. The globular isomer of cAuIB-4 and the ribbon isomer of acyclic AuIB were synthesized using selective protection of the cysteine residues with *S*-acetamidomethyl groups as described previously (19).

NMR spectroscopy

Samples for NMR contained ~2–3 m*M* peptide in ^2H_2O or 95% H_2O/5% ^2H_2O at pH 3–5.5. Total correlation spectroscopy (TOCSY), nuclear overhauser enhancement spectroscopy (NOESY), double quantum filtered correlation spectroscopy (DQF-COSY), and exclusive correlation spectroscopy (ECOSY) spectra were acquired on Bruker Avance 600 MHz or 750 MHz spectrometers as described previously (10). Briefly, the homonuclear spectra recorded included DQF-COSY, TOCSY, using a MLEV17 spin lock sequence with an isotropic mixing time of 80 ms, ECOSY, and NOESY, with mixing times of 150, 250, and 350 ms. In DQF-COSY and ECOSY experiments, the water resonance was suppressed by low-power irradiation during the relaxation delay. For the TOCSY and NOESY experiments, water suppression was achieved using a modified water suppression by gradient-tailored excitation (WATERGATE) sequence. Two-dimensional spectra were generally collected over 4096 data points in the f2 dimension and 512 increments in the f1 dimension over a spectral width of 12 ppm. Spectra were analyzed and assigned using the program XEASY (15), using the well-established sequential assignment protocol (34).

Structure calculations

Cross-peaks in NOESY spectra recorded in 95% H_2O/5% ^2H_2O with mixing times of 250 ms were integrated and calibrated in XEASY, and distance restraints were derived using CYANA (17). Backbone dihedral angle restraints were derived from $^3J_{HNH\alpha}$ coupling constants measured from line shape analysis of antiphase cross-peak splitting in the DQF-COSY spectrum. Angles were restrained to $-120^\circ \pm 30^\circ$ for $^3J_{HNH\alpha} > 8.5$ Hz and to $-60^\circ \pm 30^\circ$ for $^3J_{HNH\alpha} < 5$ Hz. Stereospecific assignments of β-methylene protons and $\chi 1$ dihedral angles were derived from $^3J_{\alpha\beta}$ coupling constants, measured from ECOSY spectra, in combination with NOE peak intensities. Preliminary structures were calculated using a torsion

angle simulated annealing protocol within CYANA, and final structures were calculated using simulated annealing and energy minimization protocols within CNS as described previously (29). Structures were analyzed using PROMOTIF and PROCHECK (18, 21).

Stability assays

The thiol stability of the peptides was assessed using reduced glutathione as described previously (3). Briefly, peptide samples (0.25 m*M*) were dissolved in a solution containing 0.25 m*M* reduced glutathione in 100 m*M* phosphate buffer and 1 m*M* EDTA (pH 7.2) and incubated at 37°C. Aliquots were taken at various time intervals, quenched with 4% TFA, and analyzed by reverse-phase HPLC (RP-HPLC) to determine if disulfide scrambling had occurred.

Serum stability assays were carried out in 100% human male serum (Sigma) using a 20 μM final peptide concentration. Serum was centrifuged at 14,000 g for 10 min to remove the lipid component, and the supernatant was incubated at 37°C for 15 min before the assay. Each peptide was incubated in serum at 37°C and 40 μl triplicate aliquots were taken out at time points 0, 3, 6, 8, and 21 h. Each serum aliquot was quenched with 40 μl of 6 *M* urea and incubated for 10 min at 5°C. Then, 40 μl of 20% trichloroacetic acid was added to each serum aliquot and incubated for another 10 min at 5°C to precipitate serum proteins. The samples were centrifuged at 14,000 g for 10 min, and 100 μl of the supernatant was analyzed on RP-HPLC using a linear gradient of solvent B (0.3 ml/min flow rate). The percentage recovery of peptides was detected by integration at 215 nm.

Biological assays

Plasmids with cDNA encoding the rat α3 and β4 nAChR subunits were obtained from J. Patrick (Baylor College of Medicine). All oocytes were injected with a total of 5 ng of cRNA and then kept at 18°C for 2–5 days before recording in ND96 buffer (96 m*M* NaCl, 2 m*M* KCl, 1.8 m*M* $CaCl_2$, 1 m*M* $MgCl_2$, and 5 m*M* HEPES at pH 7.4) supplemented with 50 mg/L gentamycin, 5 m*M* pyruvic acid, and 5% horse serum. Electrodes were pulled from borosilicate glass (Harvard Apparatus Ltd.) and had resistances of 0.3–1.5 MΩ after filling with 3 *M* KCl. All experiments were performed at room temperature (21°C–23°C). Oocytes expressing $\alpha 3\beta 4$ nAChRs were voltage clamped at −80 mV and membrane current was recorded using a two-electrode voltage virtual ground circuit on a GeneClamp 500B amplifier (Molecular Devices) or an automated workstation with eight channels in parallel, including drug delivery and on-line analysis (OpusXpress 6000A workstation; Molecular Devices). Data were digitized at 500 Hz and low-pass filtered at 200 Hz. During recordings, oocytes were perfused continuously at a rate of 2–3 ml/min, with 300 s incubation for the conopeptide. Acetylcholine (ACh; 50–100 μM) was applied for 2 s at 5 ml/min, with 3–10-min washout periods between applications, and peptides were bath applied and coapplied with the agonist. Peak current amplitude was measured before and following incubation of the peptides. All electrophysiological data were pooled ($n = 3$–7 for each data point) and represent arithmetic means ± standard error of the mean. Concentration–response curves for antagonists were fitted by unweighted nonlinear regression to the logistic equation: $E_x = E_{max}\, X^n/(X^n + IC_{50}{}^n)$, where E_x is the response, X is the antagonist concentration, E_{max} is the maximal response, n is the slope factor, and IC_{50} is the antagonist concentration that gives half-maximal inhibition of the agonist response. Curves were fitted with SigmaPlot 8.0 (Jandel Corporation). A one-way analysis of variance was used to compare modified and nonmodified conotoxins.

Results

A series of AuIB analogs were synthesized using *t*-butoxycarbonyl (Boc) chemistry and cleaved from the resin with hydrogen fluoride. A list of the sequences is given in Figure 2; both the ribbon and globular disulfide isomers were made for each AuIB analog. The cyclic analogs of AuIB are denoted cAuIB, followed by a number corresponding to the number of residues in the linker used to join the N- and C-termini. The peptides were oxidatively folded in 20% isopropanol/80% ammonium bicarbonate buffer (~pH 8). For the cyclic peptides, both cyclization and oxidation were achieved in one step using conditions outlined previously (8). The disulfide isomers were purified by RP-HPLC and analyzed by mass spectrometry and NMR to confirm their disulfide connectivity. For all sequences the ribbon isomer eluted earlier on RP-HPLC than the globular isomer, but the relative proportions of globular and ribbon isomers varied significantly for the different peptides synthesized, as shown in Figure 3. The ribbon isomers gave broader peaks on RP-HPLC than the globular isomers, suggesting the presence of multiple conformations in exchange with each other for the ribbon isomers. The beads isomer (Cys^{I}-Cys^{II}, Cys^{III}-Cys^{IV}) was not detected in any of the chromatograms.

NMR assignments of the purified peptides were made using established techniques (34) and a complete sequential assignment was obtained for all peptides. The assignments were compared with those reported previously for the corresponding acyclic peptides (12). From this analysis it was clear that the cyclic globular and ribbon forms had very similar αH NMR chemical shifts to their respective acyclic forms, as shown in Figure 4. All globular isomers of cAuIB (and linear, native AuIB) had trans conformations for all Pro residues in the structures, whereas all ribbon isomers of cAuIB differed by having a cis conformation for the peptide bond preceding Pro7.

In general, the ribbon isomers had a smaller dispersion of chemical shifts of peaks in the amide region of the NMR spectra than the globular isomers, suggesting less well-defined structures for the ribbon isomers. Spectra were recorded at pH 3.5 and 5.5 to determine if pH-dependent

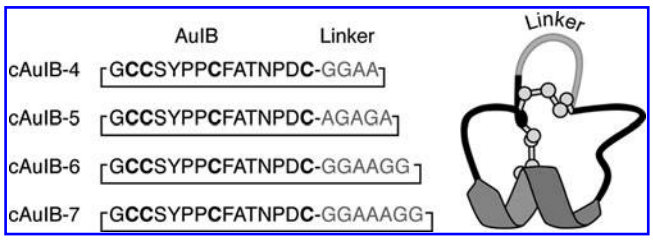

FIG. 2. Sequences of cyclic analogs of AuIB. The linker sequences used to cyclize AuIB are shown on the left and represented schematically in terms of the three-dimensional structure on the right.

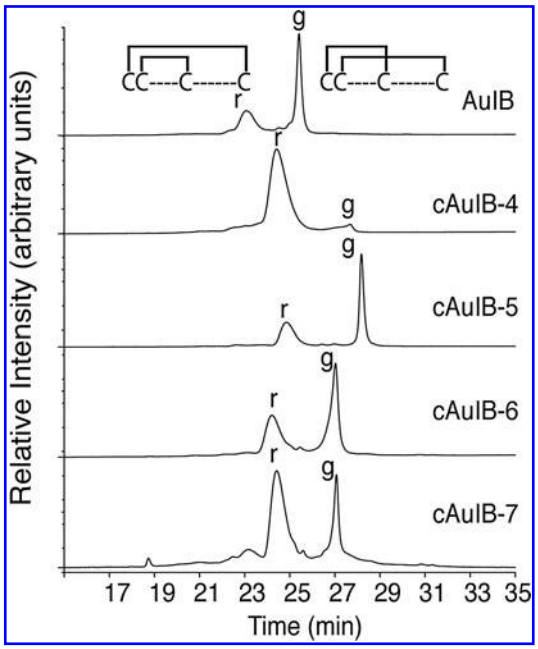

FIG. 3. Oxidative folding of AuIB and cyclic analogs. Reverse-phase high-performance liquid chromatograph showing the ribbon isomers eluting earlier than the globular isomers (globular and ribbon are referred to as g and r, respectively). The percentages of the isomers vary significantly throughout the analogs.

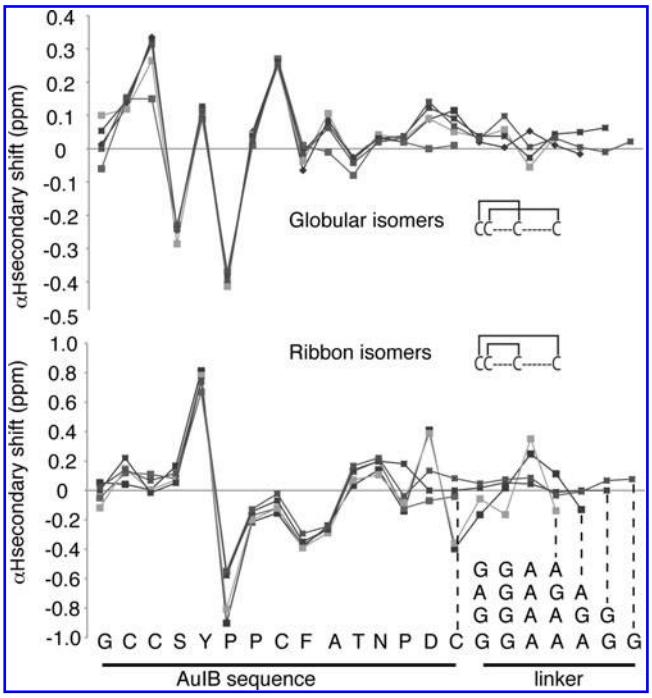

FIG. 4. Secondary αH chemical shifts of AuIB and cyclic analogs. The secondary αH shifts were calculated by subtracting the random coil shifts (33) from the experimental αH shifts. The globular isomers are shown on top and the ribbon isomers on the bottom.

structural changes were present, but no significant differences in chemical shifts were observed (data not shown), suggesting that the global folds were unaffected by pH. Therefore, the 3D structures for the globular isomers of cAuIB-4, cAuIB-5, and cAuIB-6 were determined at pH 3.5, where the exchange of the amide protons is slower than at higher pH and high-quality spectra could be obtained. Structures were not calculated for the ribbon isomers because their spectra generally contained fewer NOEs than the globular isomers, consistent with a high degree of conformational flexibility. In support of this flexibility, a trial structure calculation for the ribbon form of cAuIB-5 gave a disordered ensemble of structures, similar to that reported previously for acyclic ribbon AuIB (12).

Families of 50 structures were calculated for the globular isomers using a torsion angle dynamics protocol within CNS (6), using procedures described previously (9). A summary of the geometric and energetic statistics for the globular isomers of cAuIB-4, cAuIB-5, and cAuIB-6 is given in Table 1. The 20 lowest energy structures were chosen as the final ensembles and the structures had no NOE violations of >0.3 Å and no dihedral violations of $>3^\circ$. In all globular structures, residues six to nine form an α-helix characteristic of α-conotoxins (28). The structures had pairwise root mean square differences (RMSDs) of 0.48, 0.28, and 2.30 Å over the backbone atoms for globular cAuIB-4, cAuIB-5, and cAuIB-6, respectively. These backbone RMSDs decreased to 0.23 and 1.10 Å, for the globular isomers of cAuIB-4 and cAuIB-6, respectively, when the overlay was done over residues 1–15 (*i.e.*, the native sequence). The decreased RMSD when only the native residues of the cyclic peptides are overlaid indicates that the disorder in these cyclic peptides is primarily located in the linker region. In contrast, when the 20 lowest structures of globular cAuIB-5 are overlayed over only the native residues, the RMSD is only reduced to 0.24 Å over the backbone, which suggests that the linker region is relatively ordered in this peptide. The well-defined structure of the linker region contrasts to the somewhat disordered linkers seen in other cyclic conotoxins (8, 23), suggesting that this particular linker is structurally well tolerated in AuIB.

Figure 5 shows backbone superimpositions of ensembles of the 20 lowest energy structures of globular cAuIB-4, cAuIB-5, and cAuIB-6, oriented to display the native α-helix region (Pro6-Phe9). The structures have good covalent geometry, indicated by only small deviations from ideal bond lengths and bond angles.

Peptide stability

Incubation of the globular isomers of cyclic and linear AuIB analogs in a glutathione buffer generally resulted in disulfide bond shuffling preferentially to the ribbon isomer. The presence of the beads isomer, which contains a vicinal disulfide bond, was not observed in these experiments, and in subsequent analyses only the presence or absence of the globular and ribbon isomers was analyzed. Similar to the analytical RP-HPLC traces of the purified peptides following oxidation/cyclization, the globular isomers resulted in sharp peaks, whereas the ribbon isomers resulted in broad peaks. To determine the degree of disulfide bond shuffling, the area under each peak (recorded at $\lambda = 214$ nm) was calculated and the proportion of parent isomer remaining was determined, as shown in Figure 6. In these experiments there was a significant difference between the disulfide shuffling of the ribbon isomers and the globular isomers: the globular isomers

Table 1. Structure Statistics for Globular Isomers of Cyclic AuIB Analogs

	cAuIB-4	*cAuIB-5*	*cAuIB-6*
Experimental restraints			
Sequential NOEs	75	67	43
Medium range NOEs	43	22	30
Long range		21	11
Dihedral angles	19	15	14
Mean RMSDs from experimental restraints[a]			
NOE distances (Å)	0.009 ± 0.001	0.04 ± 0.22	0.04 ± 0.003
Dihedral angles (°)	0.24 ± 0.14	0.45 ± 0.17	0.34 ± 0.24
Mean RMSDs from idealized covalent geometry			
Bonds (Å)	0.003 ± 0.0003	0.003 ± 0.0003	0.004 ± 0.0002
Angles (°)	2.06 ± 0.04	0.49 ± 0.04	0.52 ± 0.06
Impropers (°)	0.14 ± 0.02	0.37 ± 0.05	0.35 ± 0.07
Mean energies (kcal/mol)			
E_{NOE}	6.26 ± 2.8	10.28 ± 1.2	8.33 ± 1.2
E_{DIH}	0.14 ± 0.14	0.21 ± 0.16	0.13 ± 0.18
E_{BOND}	2.32 ± 0.40	2.80 ± 0.53	3.18 ± 0.43
E_{ANGLE}	13.96 ± 1.8	16.13 ± 2.55	18.55 ± 4.3
$E_{IMPROPER}$	2.15 ± 0.33	2.84 ± 0.86	2.60 ± 1.1
E_{VDW}	-30.64 ± 3.8	-40.54 ± 3.6	-24.42 ± 7.5
Atomic RMSDs (Å)[b]			
Backbone atoms (residues 1–15)	0.23 ± 0.11	0.28 ± 0.18	1.10 ± 0.47
Heavy atoms (residues 1–15)	0.61 ± 0.17	0.84 ± 0.27	1.58 ± 0.45
Ramachandran statistics (%)[c]			
Residues in most favored regions	93.8	92.7	61.5
Residues in additionally allowed regions	6.2	7.3	38.5
Residues in generously allowed regions	0	0	0
Residues in disallowed regions	0	0	0

[a]The values are the mean ± standard deviation.
[b]Atomic RMSDs are the pairwise root mean square differences for the family of structures.
[c]Procheck NMR was used to calculate the Ramachandran statistics for residues 1–15.
NMR, nuclear magnetic resonance; NOE, nuclear overhauser enhancement.

shuffled and reached equilibrium with a majority of ribbon isomer present, whereas the ribbon isomers underwent very little disulfide shuffling. Of all the analogs, ribbon cAuIB-4 underwent the least amount of glutathione-assisted disulfide bond shuffling, retaining nearly 100% of the starting isomer after 10 h. Conversely, globular cAuIB-6 underwent the most glutathione-assisted shuffling, with only ~20% of the parent isomer remaining after 10 h. Interestingly, acyclic globular AuIB underwent significantly more disulfide bond shuffling than the cyclic peptides having five- or seven-residue linkers.

Serum stability

The stability in human serum of AuIB and its analogs was investigated to determine the effects of disulfide connectivity and backbone cyclization. RP-HPLC was used to determine the extent of degradation of the peptides, and all of the cyclic peptides were stable in human serum over a 24-h period, as shown in Figure 6. The linear form with the native, globular connectivity was also stable, but the ribbon isomer was significantly degraded. After 8 h, only ~40% of the linear ribbon AuIB remained, decreasing to <5% after 24 h. Thus, the globular connectivity is stable in human serum, and cyclization stabilizes the ribbon conformer to degradation.

Electrophysiological recordings in Xenopus oocytes

The activities of cyclized analogs of AuIB α-conotoxins on ACh-evoked currents were examined and compared with AuIB. Globular AuIB reversibly inhibited ACh-evoked currents mediated by $\alpha 3\beta 4$ nAChRs with an IC_{50} of $2.5 \pm 0.6\ \mu M$ ($n = 7$) and a Hill coefficient of 1.5 (Fig. 7A). Globular cAuIB analogs with linkers ranging from four to seven amino acids all exhibited varying degrees of inhibition, with cAuIB-5 having an apparent IC_{50} of $9.1 \pm 2.6\ \mu M$ ($n = 7$) and a Hill coefficient of 0.9. At the maximum concentration ($10\ \mu M$) tested, AuIB inhibited the ACh-evoked current by >95%, whereas cAuIB-5 inhibited the peak current amplitude by only ~50%. We were unable to determine IC_{50} values for other cAuIB analogs owing to limited material. A direct comparison of the inhibition of $\alpha 3\beta 4$ nAChRs by globular cAuIB analogs was carried out at a fixed concentration of $3\ \mu M$. AuIB reduced the ACh-evoked current amplitude to $50\% \pm 13\%$ ($n = 4$) of the control peak amplitude ($p < 0.05$), compared with cAuIB-4, cAuIB-5, cAuIB-6, and cAuIB-7, which reduced the currents to $65\% \pm 6\%$ ($n = 4$, $p < 0.05$), $81\% \pm 3\%$ ($n = 3$, $p = 0.07$), $93\% \pm 6\%$ ($n = 4$, $p = 0.3$), and $90\% \pm 7\%$ ($n = 4$, $p = 0.5$) of control current amplitude, respectively (Fig. 7B).

Cyclic ribbon AuIB analogs were compared with acyclic ribbon AuIB at a fixed concentration of $10\ \mu M$. Preincubation with the acyclic ribbon AuIB reduced $\alpha 3\beta 4$ nAChR-mediated current amplitude to $55\% \pm 2\%$ ($n = 6$) of control ($p < 0.05$) (Fig. 8A). Preincubation with cAuIB-4 reduced ACh-induced currents to $78\% \pm 3\%$ of control ($n = 3$, $p < 0.05$), whereas cAuIB-5, cAuIB-6, and cAuIB-7 did not change the current amplitude significantly, that is, $113\% \pm 6\%$ ($n = 3$, $p = 0.2$),

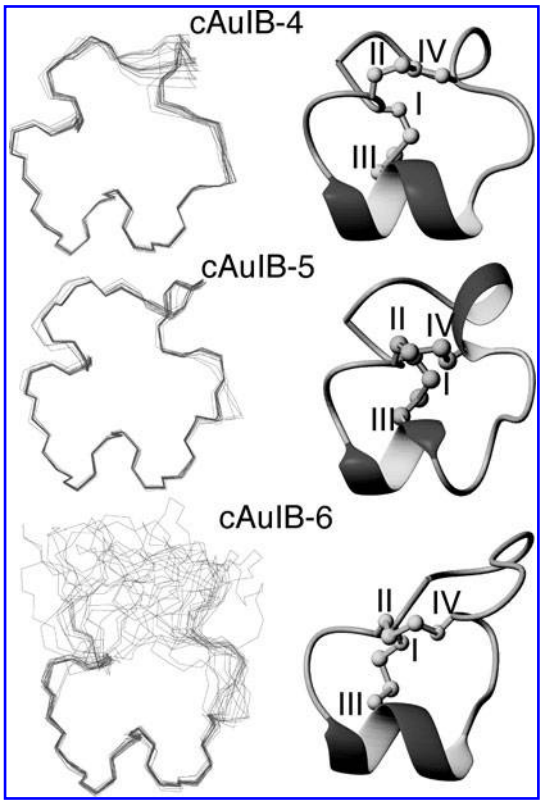

FIG. 5. Three-dimensional structures of cAuIB-4, cAuIB-5, and cAuIB-6. A superposition of the 20 lowest energy structures is shown on the left with the corresponding secondary structure representations on the right. Structures were determined using nuclear magnetic resonance spectroscopy; the four cysteine residues are numbered with Roman numerals, the disulfide bonds are shown in ball and stick format, and the helixes are shown as thickened ribbons.

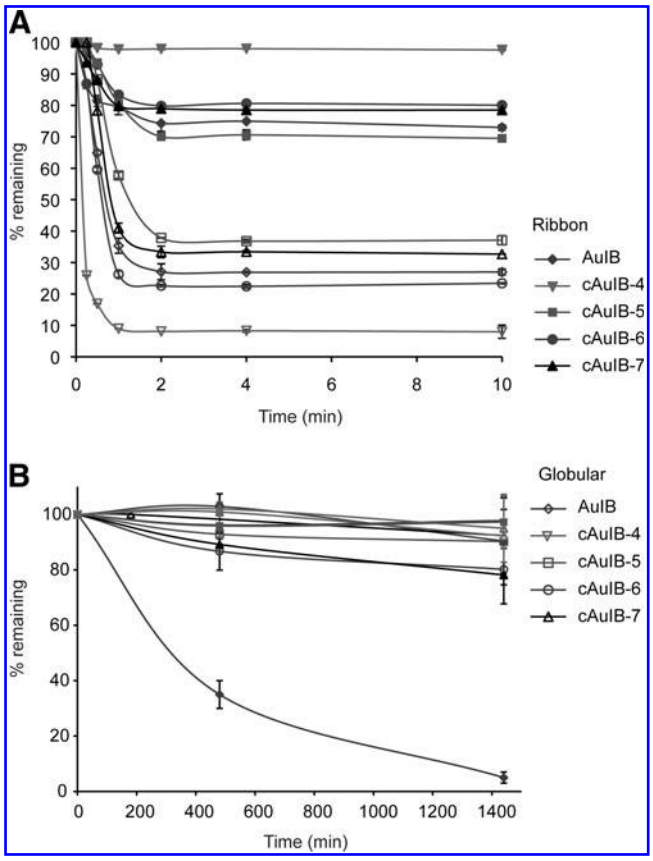

FIG. 6. Disulfide and serum stability of AuIB and cyclic analogs. (**A**) AuIB and the cyclic analogs were incubated in glutathione solution (see Materials and Methods section) and the proportion (expressed as a percentage) of the original isomer is plotted relative to time. (**B**) Stability of AuIB analogs in human serum. The stability of the peptides in human serum was determined over a 24-h period. All analogs were stable with the exception of the acyclic ribbon isomer.

93% ± 2% ($n = 3$, $p = 0.1$), and 98% ± 2% ($n = 4$, $p = 0.3$) of control values, respectively (Fig. 8B). Inhibition of ACh-evoked currents by cAuIB-4 was significantly less compared with the acyclic ribbon AuIB ($n = 3$, $p < 0.01$).

Discussion

In the present study we synthesized cyclic forms of α-conotoxin AuIB using native chemical ligation, with linker sizes ranging from four to seven residues. Cyclization has been shown to be useful in stabilizing conotoxins and enhancing their therapeutic potential (8, 23). However, the effectiveness of this technique on a range of conotoxins and, in particular, the influences of cyclization on structure and stability have not been fully explored. In the present study we analyzed the oxidative folding, 3D structures, and disulfide and serum stability of cyclic forms of AuIB compared with acyclic forms, all of which have provided insights into factors influencing the stability of AuIB. Disulfide bond stability *in vivo* is a potential limitation in the use of disulfide-rich peptides as drugs, given that glutathione is present in blood in high concentrations and can facilitate disulfide bond exchange (3, 26, 31). Therefore, understanding the factors influencing the disulfide stability of α-conotoxins should be useful in studies aimed at exploiting their therapeutic potential.

Significant differences were observed in the oxidative folding reactions of AuIB and its cyclic analogs. Under the folding conditions used in this study, which did not involve directed disulfide formation, the major product of oxidative folding of the reduced acyclic peptide was the globular isomer (Fig. 2). However, on oxidation of the reduced cyclic analogs, the proportions of the resulting globular or ribbon isomers varied considerably with linker size. The smallest linker used (four residues in cAuIB-4) resulted predominately in ribbon isomer. For this analog the yield of the globular isomer was so low that selective protection of the disulfide bonds in a separate synthesis was required for its isolation. By contrast, both globular and ribbons isomers were isolated from the nondirected oxidation of cAuIB-5, cAuIB-6, and cAuIB-7, with an increasing amount of ribbon isomer obtained as the linker length was increased (Fig. 2).

Given that the length of the linker appeared to be influencing the oxidative folding outcomes for the cyclic AuIB analogs, it was of interest to determine their structures to establish the reason for this influence. Three-dimensional

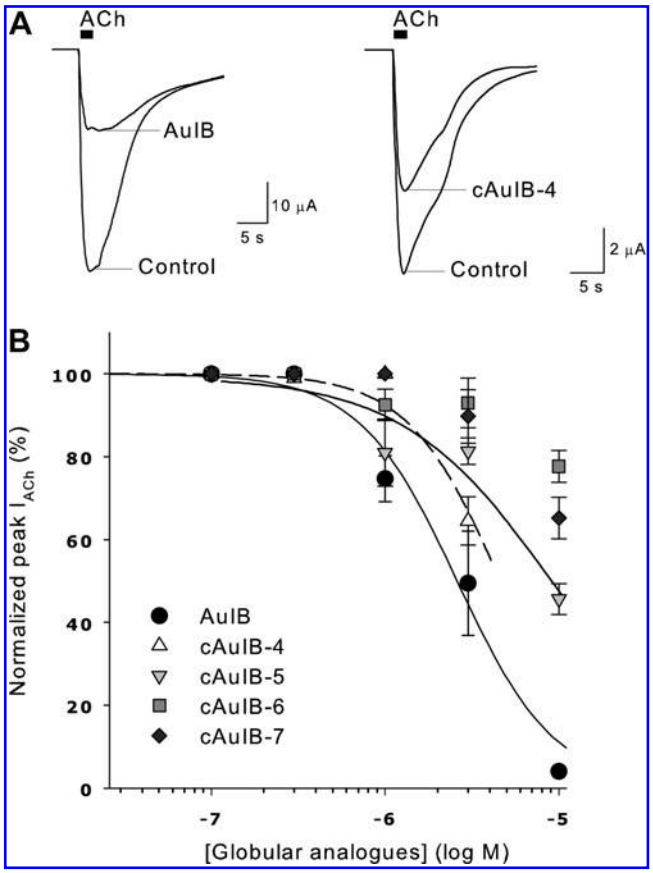

FIG. 7. Electrophysiological assays of globular AuIB analogs at α3β4 nAChRs expressed in *Xenopus* oocytes. (**A**) Representative ACh-evoked currents obtained in the absence (control) and presence of 3 μM AuIB (globular) and cAuIB-4 (globular). (**B**) Concentration–response relationships obtained for the inhibitory effects of AuIB (globular) analogs.

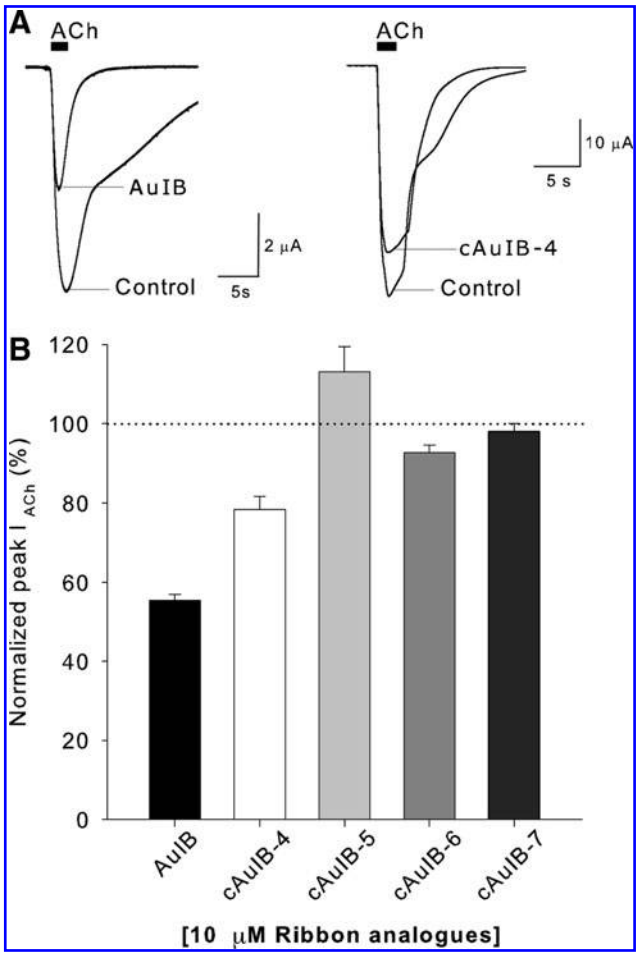

FIG. 8. Electrophysiological assays of ribbon AuIB analogs at α3β4 nAChRs expressed in *Xenopus* oocytes. (**A**) Representative ACh-evoked currents obtained in the absence (control) and presence of AuIB (ribbon) and cAuIB-4 (ribbon) (10 μM). (**B**) Bar graph of normalized peak current amplitudes showing comparison of inhibitory effects of AuIB [ribbon] analogs tested at 10 μM concentration.

structures of the cyclic ribbon isomers were not determined because of a relative lack of NOEs to define their structures. The small number of NOEs is likely to be a consequence of flexibility in the ribbon isomers. However, the 3D structures of the globular isomers of cAuIB-4, cAuIB-5, and cAuIB-6 were determined and it was found that a well-defined characteristic α-conotoxin fold is maintained in all three analogs. The linker for cAuIB-6 is more disordered than for the analogs with shorter linkers, presumably as a result of flexibility in this region of the structure. Although the structure of cAuIB-7 was not determined, the residues in the linker region have αH chemical shifts very close to random coil (Fig. 4), consistent with the linker being disordered in this peptide as well. The higher disorder in the structures as the linker size increases correlates with a higher production of ribbon isomer with increasing linker size, suggesting that the disordered linkers might preferentially destabilize the globular form. However, this explanation is inconsistent with the high proportion of ribbon isomer formed in the oxidative folding of cAuIB-4, where the linker is well defined. Overall, the five-residue linker was optimal for forming the globular isomer under the *in vitro* folding conditions used in the present study.

An electrophysiological study of α3β4 nAChRs expressed in oocytes indicated that cyclization of either globular or ribbon AuIB reduces their potency relative to the acyclic forms. The potency of the cyclized AuIB analogs decreases with increasing linker length such that ribbon cAuIB-7 exhibits no effect on ACh-induced currents, and globular cAuIB-7 shows only minimal activity.

The ribbon cAuIB analog, cAuIB-4, inhibited (~20%) α3β4 nAChRs at a concentration of 10 μM, whereas the other ribbon analogs were all inactive. In contrast, the inhibition was more pronounced with cyclic globular cAuIB analogs tested at 3 μM. The native AuIB inhibited the ACh-evoked current by ~50% and the cyclic analogs exhibited an increase in nAChR inhibition as the linker length was shortened: from 10% inhibition observed for globular cAuIB-7 to 35% inhibition for globular cAuIB-4 at 3 μM (Fig. 7B).

The cAuIB-4 analog of both globular and ribbon isoforms was the most potent of all the cyclic analogs tested on α3β4 nAChRs. This indicates that shorter linker lengths may be optimal for cyclization of AuIB α-conotoxin. However, the reduced activity of cyclized AuIB analogs should not be generalized to all conotoxins, given that some cyclic analogs

of MII conotoxin have been previously shown to retain near full biological activity compared with nonmodified MII (8).

Analysis of the disulfide scrambling, as shown in Figure 4, revealed that all of the ribbon isomers scrambled to a lesser extent than the globular isomers. This higher stability of the ribbon isomers is surprising given the apparently disordered structures of the ribbon isomers and their nonnative disulfide connectivity. cAuIB-5 and cAuIB-7 had higher relative proportions of globular isomer remaining after incubation with glutathione than the acyclic globular isomer, indicating that cyclization can improve the stability of the globular isomer to shuffling. Interestingly, the relative proportion of globular isomer remaining after incubation with glutathione (Fig. 6) does not correlate with the relative proportions obtained in the oxidative folding reactions (Fig. 3). Further, analysis of the surface exposure of the disulfide bonds in the structures of cAuIB-4, −5, and −6 indicates that surface exposure of the disulfide bonds does not correlate with stability in the shuffling assay. Therefore, it appears that the overall fold contributes to the stability of the disulfide bonds rather than simply the surface exposure of the cysteine residues, which might be considered as a measure of access to reducing/oxidizing agents in solution.

The disulfide scrambling in glutathione has been previously examined for α-conotoxins ImI (3) and PnIA (19). Incubation of the globular isomer of ImI in a glutathione buffer resulted in shuffling to ~50% each of the globular and ribbon isomers. Analysis of the globular isomers of an analog of PnIA and truncated forms revealed that the full-length peptide with a 4/7 intercysteine spacing, and a 4/6 version, resulted in ~40% of the globular isomer left after incubation. Therefore, these variants of PnIA behave in a similar manner to that observed for the acyclic form of AuIB, which might be related to the similar loop spacings of these peptides. The globular isomers of the truncated forms of PnIA with 4/5, 4/4, and 4/3 loop spacings were very unstable in the glutathione shuffling assay and predominately converted to the ribbon isomer. This high level of shuffling contrasts with observations for ImI, which has a 4/3 loop spacing (3). Overall, the results indicate that the disulfide stability of the α-conotoxins is highly dependent on the sequence and loop spacing.

In contrast to the disulfide scrambling experiments, all of the AuIB peptides tested in the present study, with the exception of the linear ribbon isomer of AuIB, were stable in human serum. Although the ribbon isomers of the cyclic forms of AuIB appear to have disordered structures, similar to the linear form, cyclization of the backbone clearly has a significant influence on the stability of AuIB and highlights the importance of this approach in stabilizing disulfide-rich peptides. This approach has been successfully applied to α-conotoxin MII and χ-conotoxin MrIA to stabilize them (8, 23). Given that the ribbon form of AuIB is bioactive (12), stabilization by cyclization might be useful for the therapeutic use of this peptide.

Selenocysteine substitutions (3) have also been used to stabilize the disulfide bonds of conotoxins. Analogs of ImI with selenocysteine did not shuffle in glutathione in contrast to the native peptide (3). However, there might be limitations in the use of selenocysteine-containing compounds as therapeutics because of potential toxicity (2), and cyclization seems to be a preferred alternative method for stabilizing the disulfide connectivities of conotoxins.

In summary, we have shown that cyclization of AuIB influences its *in vitro* oxidative folding outcomes and that the ribbon isomers are more resistant to disulfide scrambling than the globular isomers. This is unusual considering that globular isomers are typically the native forms found in venom and are generally more potent against nAChRs. Cyclization improves the disulfide stability of the globular isomers and dramatically improves the serum stability of the ribbon isomers. The ribbon isomer for AuIB is bioactive, and therefore, stabilization of this analog might have potential therapeutic applications, where *in vivo* stability is important. Overall, these results provide insight into the disulfide stability of α-conotoxin AuIB and this information should be valuable in the design of more stable antagonists of nAChRs.

Acknowledgments

This work was supported by the Australian Research Council (ARC DP0986281) and the National Health and Medical Research Council (NHMRC). D.J.C. is an NHMRC Professonal Fellow, D.J.A. is an ARC Australian Professional Fellow, N.L.D. is a Queensland Smart State Fellow.

Author Disclosure Statement

No competing financial interests exist.

References

1. Adams DJ, Alewood PF, Craik DJ, Drinkwater RD, and Lewis RJ. Conotoxins and their potential pharmaceutical applications. *Drug Dev Res* 46: 219–234, 1999.
2. Andreadou I, van de Water B, Commandeur JN, Nagelkerke FJ, and Vermeulen NP. Comparative cytotoxicity of 14 novel selenocysteine se-conjugates in rat renal proximal tubular cells. *Toxicol Appl Pharmacol* 141: 278–287, 1996.
3. Armishaw CJ, Daly NL, Nevin ST, Adams DJ, Craik DJ, and Alewood PF. Alpha-selenoconotoxins, a new class of potent alpha7 neuronal nicotinic receptor antagonists. *J Biol Chem* 281: 14136–14143, 2006.
4. Armishaw CJ, Dutton JL, Craik DJ, and Alewood PF. Establishing regiocontrol of disulfide bond isomers of alpha-conotoxin ImI via the synthesis of N-to-C cyclic analogues. *Biopolymers* 94:307–313, 2010.
5. Azam L and McIntosh JM. Alpha-conotoxins as pharmacological probes of nicotinic acetylcholine receptors. *Acta Pharmacol Sin* 30: 771–783, 2009.
6. Brünger AT, Adams PD, and Rice LM. New applications of simulated annealing in X-ray crystallography and solution NMR. *Structure* 5: 325–336, 1997.
7. Brust A, Palant E, Croker DE, Colless B, Drinkwater R, Patterson B, Schroeder CI, Wilson D, Nielsen CK, Smith MT, Alewood D, Alewood PF, and Lewis RJ. chi-Conopeptide pharmacophore development: toward a novel class of norepinephrine transporter inhibitor (Xen2174) for pain (perpendicular). *J Med Chem* 52: 6991–7002, 2009.
8. Clark RJ, Fischer H, Dempster L, Daly NL, Rosengren KJ, Nevin ST, Meunier FA, Adams DJ, and Craik DJ. Engineering stable peptide toxins by means of backbone cyclization: stabilization of the alpha-conotoxin MII. *Proc Natl Acad Sci U S A* 102: 13767–13772, 2005.
9. Clubb RT, Ferguson SB, Walsh CT, and Wagner G. Three-dimensional solution structure of *Escherichia coli* periplasmic cyclophilin. *Biochemistry* 33: 2761–2772, 1994.

10. Daly NL, Clark RJ, Plan MR, and Craik DJ. Kalata B8, a novel antiviral circular protein, exhibits conformational flexibility in the cystine knot motif. *Biochem J* 393: 619–626, 2006.
11. Dutertre S and Lewis RJ. Toxin insights into nicotinic acetylcholine receptors. *Biochem Pharmacol* 72: 661–670, 2006.
12. Dutton JL, Bansal PS, Hogg RC, Adams DJ, Alewood PF, and Craik DJ. A new level of conotoxin diversity, a non-native disulfide bond connectivity in alpha-conotoxin AuIB reduces structural definition but increases biological activity. *J Biol Chem* 277: 48849–48857, 2002.
13. Dutton JL and Craik DJ. alpha-Conotoxins: nicotinic acetylcholine receptor antagonists as pharmacological tools and potential drug leads. *Curr Med Chem* 8: 327–344, 2001.
14. Dwoskin LP and Crooks PA. Competitive neuronal nicotinic receptor antagonists: a new direction for drug discovery. *J Pharmacol Exp Ther* 298: 395–402, 2001.
15. Eccles C, Guntert P, Billeter M, and Wüthrich K. Efficient analysis of protein 2D NMR spectra using the software package EASY. *J Biomol NMR* 1: 111–130, 1991.
16. Grishin AA, Wang CI, Muttenthaler M, Alewood PF, Lewis RJ, and Adams DJ. α-Conotoxin AuIB isomers exhibit distinct inhibitory mechanisms and differential sensitivity to stoichiometry of α3β4 nAChRs. *J Biol Chem* 285: 22254–22263, 2010.
17. Guntert P, Mumenthaler C, and Wüthrich K. Torsion angle dynamics for NMR structure calculation with the new program DYANA. *J Mol Biol* 273: 283–298, 1997.
18. Hutchinson EG and Thornton JM. PROMOTIF—a program to identify and analyze structural motifs in proteins. *Protein Sci* 5: 212–220, 1996.
19. Jin AH, Daly NL, Nevin ST, Wang CI, Dutertre S, Lewis RJ, Adams DJ, Craik DJ, and Alewood PF. Molecular engineering of conotoxins: the importance of loop size to alpha-conotoxin structure and function. *J Med Chem* 51: 5575–5584, 2008.
20. Klotz U. Ziconotide—a novel neuron-specific calcium channel blocker for the intrathecal treatment of severe chronic pain—a short review. *Int J Clin Pharmacol Ther* 44: 478–483, 2006.
21. Laskowski RA, Moss DS, and Thornton JM. Main-chain bond lengths and bond angles in protein structures. *J Mol Biol* 231: 1049–1067, 1993.
22. Livett BG, Gayler KR, and Khalil Z. Drugs from the sea: conopeptides as potential therapeutics. *Curr Med Chem* 11: 1715–1723, 2004.
23. Lovelace ES, Armishaw CJ, Colgrave ML, Wahlstrom ME, Alewood PF, Daly NL, and Craik DJ. Cyclic MrIA: a stable and potent cyclic conotoxin with a novel topological fold that targets the norepinephrine transporter. *J Med Chem* 49: 6561–6568, 2006.
24. Luo S, Kulak JM, Cartier GE, Jacobsen RB, Yoshikami D, Olivera BM, and McIntosh JM. alpha-Conotoxin AuIB selectively blocks alpha3 beta4 nicotinic acetylcholine receptors and nicotine-evoked norepinephrine release. *J Neurosci* 18: 8571–8579, 1998.
25. McIntosh JM, Santos AD, and Olivera BM. Conus peptides targeted to specific nicotinic acetylcholine receptor subtypes. *Annu Rev Biochem* 68: 59–88, 1999.
26. Meister A and Anderson ME. Glutathione. *Annu Rev Biochem* 52: 711–760, 1983.
27. Miljanich GP. Ziconotide: neuronal calcium channel blocker for treating severe chronic pain. *Curr Med Chem* 11: 3029–3040, 2004.
28. Millard EL, Daly NL, and Craik DJ. Structure-activity relationships of alpha-conotoxins targeting neuronal nicotinic acetylcholine receptors. *Eur J Biochem* 271: 2320–2326, 2004.
29. Nicke A, Loughnan ML, Millard EL, Alewood PF, Adams DJ, Daly NL, Craik DJ, and Lewis RJ. Isolation, structure, and activity of GID, a novel alpha 4/7-conotoxin with an extended N-terminal sequence. *J Biol Chem* 278: 3137–3144, 2003.
30. Nicke A, Samochocki M, Loughnan ML, Bansal PS, Maelicke A, and Lewis RJ. Alpha-conotoxins EpI and AuIB switch subtype selectivity and activity in native versus recombinant nicotinic acetylcholine receptors. *FEBS Lett* 554: 219–223, 2003.
31. Rabenstein DL and Weaver KH. Kinetics and equilibria of the thiol/disulfide exchange reactions of somatostatin with glutathione. *J Org Chem* 61: 7391–7397, 1996.
32. Terlau H and Olivera BM. Conus venoms: a rich source of novel ion channel-targeted peptides. *Physiol Rev* 84: 41–68, 2004.
33. Wishart DS, Bigam CG, Holm A, Hodges RS, and Sykes BD. ^{1}H, ^{13}C and ^{15}N random coil NMR chemical shifts of the common amino acids. I. Investigations of nearest-neighbor effects. *J Biomol NMR* 5: 67–81, 1995.
34. Wüthrich K. *NMR of Proteins and Nucleic Acids*. New York: Wiley-Interscience, 1986.
35. Yuan DD, Han YH, Wang CG, and Chi CW. From the identification of gene organization of alpha conotoxins to the cloning of novel toxins. *Toxicon* 49: 1135–1149, 2007.

Address correspondence to:
Dr. Norelle L. Daly
Division of Chemistry and Structural Biology
Institute for Molecular Bioscience
The University of Queensland
Brisbane, QLD 4072
Australia

E-mail: n.daly@imb.uq.edu.au

Date of first submission to ARS Central, December 22, 2009; date of final revised submission, April 5, 2010; date of acceptance, May 15, 2010.

Abbreviations Used

ACh = acetylcholine
Boc = *t*-butoxycarbonyl
DQF-COSY = double quantum filtered correlation spectroscopy
ECOSY = exclusive correlation spectroscopy
nAChR = nicotinic acetylcholine receptor
NMR = nuclear magnetic resonance
NOESY = nuclear overhauser enhancement spectroscopy
RMSD = root mean square difference
RP-HPLC = reverse-phase high-performance liquid chromatography
TFA = trifluoroacetic acid
TOCSY = total correlation spectroscopy
WATERGATE = water suppression by gradient-tailored excitation

This article has been cited by:

1. Sunithi Gunasekera, Teshome L. Aboye, Walid A. Madian, Hesham R. El-Seedi, Ulf Göransson. 2013. Making Ends Meet: Microwave-Accelerated Synthesis of Cyclic and Disulfide Rich Proteins Via In Situ Thioesterification and Native Chemical Ligation. *International Journal of Peptide Research and Therapeutics* **19**:1, 43-54. [CrossRef]
2. Jon-Paul Bingham, Elizabeth A. Andrews, Shaun M. Kiyabu, Chino C. Cabalteja. 2012. Drugs from Slugs. Part II – Conopeptide bioengineering. *Chemico-Biological Interactions* **200**:2-3, 92-113. [CrossRef]
3. Christina I Schroeder, David J Craik. 2012. Therapeutic potential of conopeptides. *Future Medicinal Chemistry* **4**:10, 1243-1255. [CrossRef]
4. Richard J. Clark, David J. CraikEngineering Cyclic Peptide Toxins **503**, 57-74. [CrossRef]
5. Luis M. Tuesta, Christie D. Fowler, Paul J. Kenny. 2011. Recent advances in understanding nicotinic receptor signaling mechanisms that regulate drug self-administration behavior. *Biochemical Pharmacology* **82**:8, 984-995. [CrossRef]
6. David J. Craik. 2011. The Folding of Disulfide-Rich Proteins. *Antioxidants & Redox Signaling* **14**:1, 61-64. [Abstract] [Full Text HTML] [Full Text PDF] [Full Text PDF with Links]
7. Christopher J. Armishaw, Anders A. Jensen, Lena D. Balle, Krystle C.M. Scott, Lena Sørensen, Kristian Strømgaard. 2011. Improving the Stability of α-Conotoxin AuIB Through N-to-C Cyclization: The Effect of Linker Length on Stability and Activity at Nicotinic Acetylcholine Receptors. *Antioxidants & Redox Signaling* **14**:1, 65-76. [Abstract] [Full Text HTML] [Full Text PDF] [Full Text PDF with Links]